Current Chemistry Letters 13 (2024) 325–334

Contents lists available at GrowingScience

Current Chemistry Letters

homepage: www.GrowingScience.com

Development of a novel hyperbranched unsaturated polyester resin: Synthesis, characterization, and potential applications in car body putty

Mohammad Abdollahi[a] and Behzad Khalili[a*]

[a]*University of Guilan, Faculty of Sciences, Department of Chemistry, Rasht, Iran*

C H R O N I C L E

Article history:
Received March 20, 2023
Received in revised form
June 17, 2023
Accepted November 8, 2023
Available online
November 8, 2023

Keywords:
Unsaturated polyester resin
Modified dehydrated castor oil fatty acid
Dicyclopentadiene maleate
Trimethylolpropane diallyl ether
Car body putty

A B S T R A C T

This work presents a comprehensive synthesis method for the development of a new hyperbranched unsaturated polyester resin (HUPR). The resin is synthesized by modifying dehydrated castor oil fatty acid (DCOFA) with methyl methacrylate (MMA) and styrene, dicyclopentadiene-maleate (DCPD-M), and trimethylol propane diallyl ether (TMPDE). The synthesis process involves the radical addition reaction of DCOFA with MMA and styrene, followed by the addition of DCPD-M and TMPDE to form a HUPR. The resulting resin exhibits enhanced properties, making it a promising candidate for car body putty in the polymer industry.

1. Introduction

Hyperbranched polyester resins (HPR)[1-4] are a type of highly branched polymer that exhibit exceptional physical and chemical properties. These resins are synthesized through a unique polymerization process, resulting in a three-dimensional network structure with numerous branches. They can be easily applied as coatings on various surfaces, providing a protective barrier against external factors such as moisture, chemicals, and physical damage[5-8]. Unsaturated polyester resin (UPR), commonly used in various applications such as coatings, adhesives, and composites, can also be classified as a HPR. Unlike linear polyesters, HPRs possess a highly branched molecular structure, resulting in unique properties and enhanced performance characteristics[9]. UPRs are a class of versatile polymers that have gained significant attention in the field of polymer chemistry due to their wide range of applications. These polymers are synthesized through the reaction of unsaturated dibasic acids or anhydrides with diols or polyols[10-12], resulting in a polyester backbone with unsaturated bonds. The presence of these unsaturated bonds provides reactivity and flexibility to UPRs, making them suitable for various applications in industries such as automotive, construction, and electronics.

The synthesis of UPRs involves a two-step process: the esterification of the dibasic acid or anhydride with the diol or polyol, followed by the addition of a cross-linking agent, typically a monomer containing vinyl groups. The cross-linking agent reacts with the unsaturated bonds in the polyester backbone, leading to the formation of a three-dimensional network structure. This cross-linking process is often initiated by the addition of a catalyst or through thermal activation. UPRs can be categorized into different types, including flame-retardant UPR[13-15], flexible UPR[16-17], chemical-resistant UPR[18], electrical-resistant UPR[19-21], specialty UPR[22-24], and general purpose UPR[25-26]. To examine their chemical properties, techniques such as Thermogravimetric Analysis (TGA)[27], Attenuated Total Reflectance Fourier-Transform Infrared (ATR FTIR)[28], Carbon-13 nuclear magnetic resonance (^{13}C-NMR)[29], Differential Scanning Calorimetry (DSC)[30], microscopy[31-

* Corresponding author.
E-mail address B.khalili@guilan.ac.ir (B. Khalili)

doi: 10.5267/j.ccl.2023.11.006

[32], and light scattering[33] are employed. Additionally, standard test methods like ASTM D648, ISO 527-2, ASTM D2583, etc., are utilized to measure the mechanical properties of cured UPR composites.

Modification of DCOFA with MMA and styrene offers the potential for developing novel materials with improved properties. By copolymerizing these monomers with DCOFA, the resulting polymers can exhibit enhanced drying and flexibility[34]. The choice of monomers allows for the customization of the copolymer to meet specific requirements in various industries. In present work, in addition to modified DCOFA, DCPD-M[35] and TMPDE are other components used in UPR synthesis. It further enhances the mechanical properties of resin[34], including its hardness and toughness. This combination of ingredients results in a UPR that exhibits excellent performance in various applications, such as automotive parts, construction materials, and electrical components.

2. Results and Discussion

The comprehensive synthesis method described in this work successfully yielded a new HUPR. The resin was synthesized by modifying DCOFA with MMA and styrene (Intermediate A), DCPD-M (Intermediate B) and TMPDE. The first step of the synthesis process involved the radical addition of MMA and styrene to DCOFA. This reaction resulted in the formation of an intermediate that served as the base for further modifications. The radical addition reaction was carefully controlled to ensure the desired degree of conversion and purity of the intermediate A (**Scheme 1**).

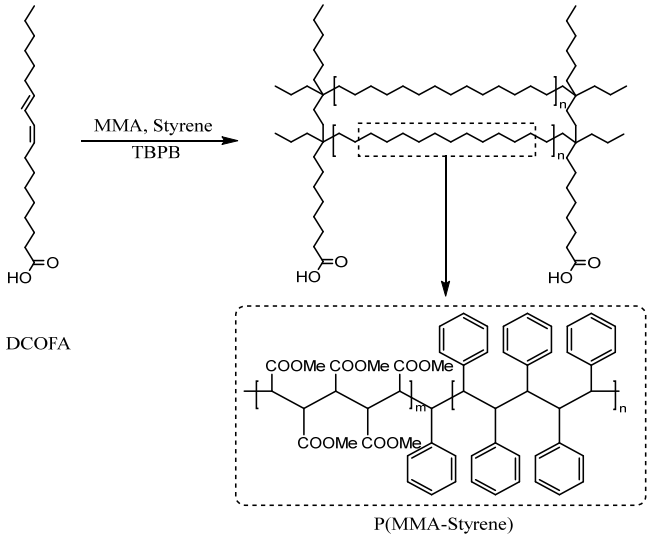

Scheme 1. Proposed structure for Intermediate A

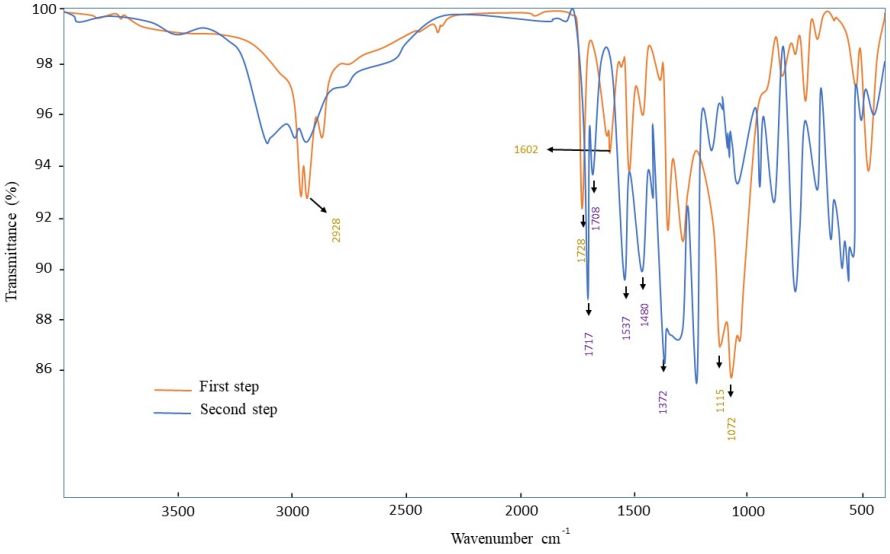

Fig. 1. FTIR spectrum of first and second step

The FTIR spectrum of the synthesized product provides valuable insights into the chemical transformations that occurred during the first step of the process (**Fig. 1**). Upon analysis of the FTIR spectrum, a notable change is observed in the region corresponding to the unsaturated bonds of DCOFA. Prior to the radical addition reaction, DCOFA exhibited characteristic peaks associated with these unsaturated bonds (1602 cm^{-1}). However, after the reaction with MMA and styrene, these peaks disappear. This indicates that the unsaturated bonds of DCOFA have undergone a reaction with the added monomers, resulting in their elimination or conversion into new chemical entities. The disappearance of the peaks associated with the unsaturated bonds of DCOFA suggests successful incorporation of MMA and styrene into the intermediate product. This transformation is crucial for the subsequent modifications and desired properties of the synthesized material. The careful control of the radical addition reaction ensures the desired degree of conversion and purity of the intermediate product, as evidenced by the changes observed in the FTIR spectrum. The synthesis of DCPD-M (Intermediate B) involves the addition of maleic anhydride (MA) to water, followed by the slow and controlled addition of DCPD to the mixture. The reaction takes place at elevated temperatures and under controlled conditions to ensure the formation of the desired DCPD-M product (**Scheme 2**).

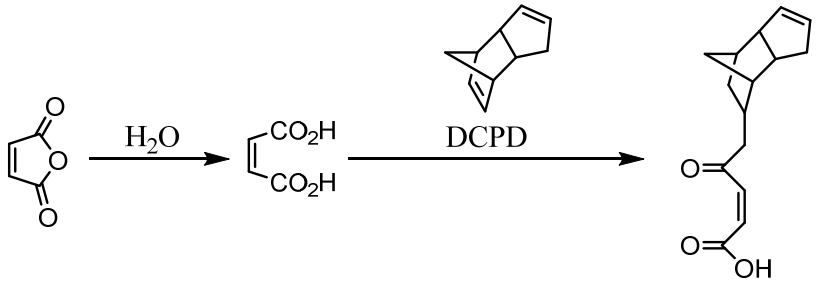

Scheme 2. Proposed structure for intermediate B

The scheme 3 presents proposed molecular structure for final UPR that incorporates specific components to enhance its performance. This HUPR is uniquely end-capped with DCPD and TMPDE double bond, imparting distinct properties to the resin, Additionally, it incorporates modified DCOFA within its structure. The hyperbranched structure of the UPR provides enhanced mechanical properties, such as improved tensile strength and impact resistance. The incorporation of DCPD and TMPDE as end-capping agents will further enhance the crosslinking density, resulting in increased chemical resistance and thermal stability.

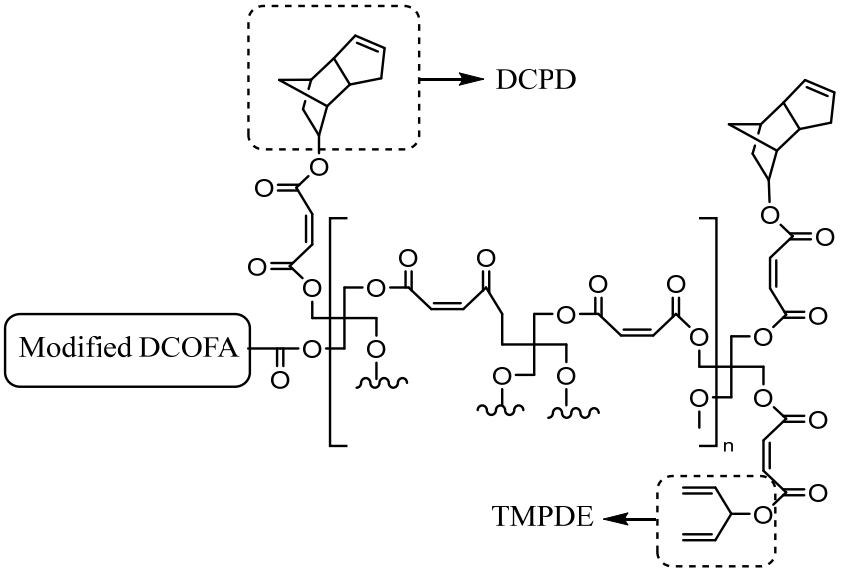

Scheme 3. Proposed structure for Final UPR

The IR spectrum of final UPR displays characteristic peaks indicating the presence of these functional groups. A strong peak at 1727 cm^{-1} signifies the ester group, while a peak at 1618 cm^{-1} suggests the presence of aliphatic unsaturated bonds (**Fig. 2**). In this step DCPD-M and (TMPDE) were added to the reaction mixture. These additions led to the formation of crosslinking sites within the resin structure, enhancing its mechanical and thermal properties (**Scheme 3**).

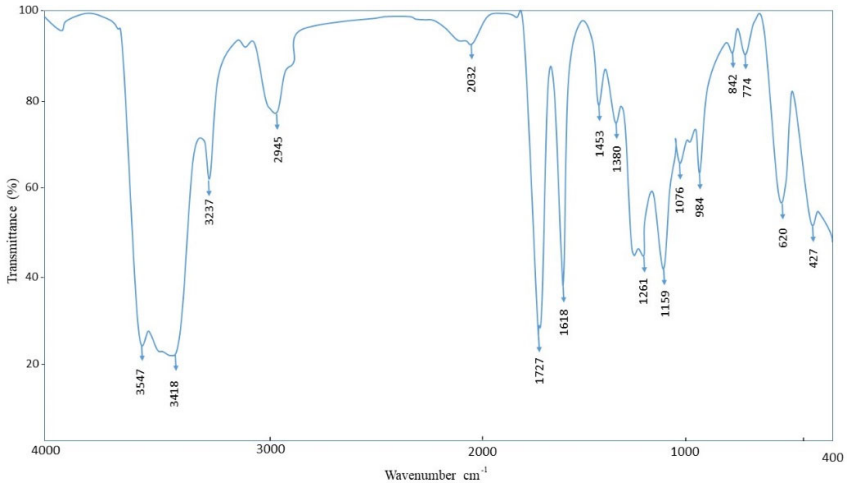

Fig. 2. FTIR spectrum of final UPR

GPC (Gel Permeation Chromatography)

Fig. 3 represents a GPC graph of the final UPR, with the y-axis representing viscosity molecular weight (Mv) and the x-axis representing time in min. The results of the GPC test, conducted on the final UPR, reveal interesting findings regarding the molecular weight distribution. The evaluation shows the presence of two distinct peaks, observed at 7.5 and 9.5 min, respectively. These peaks correspond to specific molecular weights, with the first peak measuring 59687 daltons and the second peak measuring 1542 daltons. **Fig. 3** provides a visual representation of these findings. The graph illustrates the intensity of particles at different molecular weights, with the two prominent peaks clearly visible. Furthermore, the results indicate that the UPR sample contains a variety of particles with different molecular weights. This diversity is particularly noticeable in the lower molecular weight range, which corresponds to the second peak. The presence of numerous particles in this range suggests a wider distribution of molecular weights and may have implications for the resin's properties and performance.

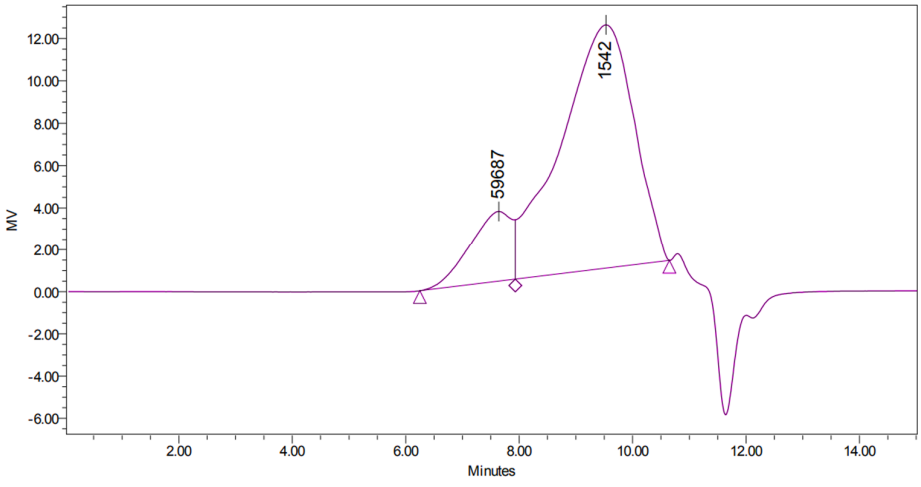

Fig. 3. GPC graph of final UPR

Scanning Electron Microscopy (SEM)

The SEM image of the UPR reveals a highly uniform and smooth surface, indicative of its exceptional quality for car putty application (**Fig. 4**). The resin matrix exhibits a dense and compact microstructure, with minimal porosity or voids. This microstructure is crucial for achieving high tensile strength and durability, which are essential for automotive repair purposes.

The observed microstructure in the SEM image suggests that the UPR possesses excellent mechanical properties, making it suitable for car putty applications. The absence of porosity or voids indicates enhanced resistance to environmental factors, such as moisture and temperature fluctuations, which are commonly encountered in automotive environments. These properties are crucial for ensuring long-term performance and stability when used for repairing car surfaces.

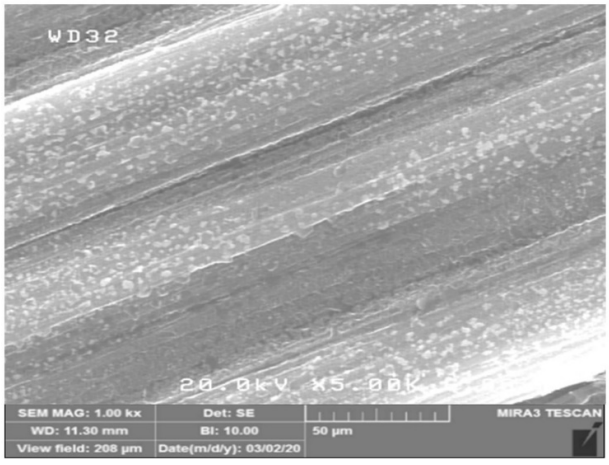

Fig. 4. SEM image of final UPR

Dynamic Mechanical Analysis (DMA)

DMA is a technique used to analyse the mechanical properties of materials, including UPR. In recent study, DMA was employed to compare the behavior of neat UPR (without fillers) and reinforced UPR (**Fig. 5**). The results of the analysis revealed that the storage modulus of the reinforced UPR was higher than that of the neat UPR. This indicates that the presence of fillers enhanced the stiffness and rigidity of the UPR.

This difference in storage modulus can be attributed to the presence of reinforcing materials such as talk, aerosil or other fillers in reinforced UPR. These reinforcing materials enhance the mechanical properties of the UPR, resulting in a higher storage modulus.

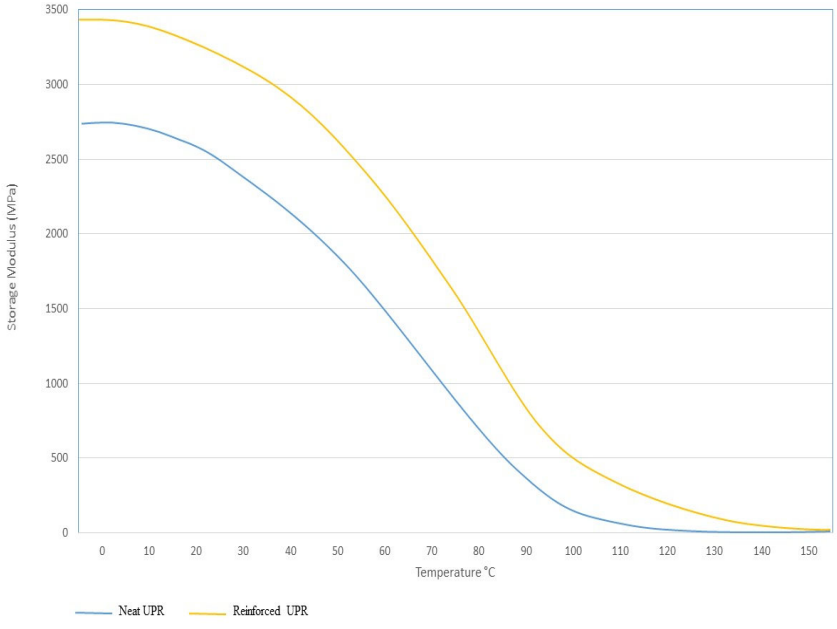

Fig. 5. DMA graph of final UPR

Wetting angle measurements (Contact angle)

In a recent study, it was found that a contact angle of 75.1 degrees in a wetting test indicates an intermediate state between hydrophobicity and hydrophilicity in presented UPR (**Fig. 6**). This angle is a crucial indicator of the surface properties of the material and its ability to interact with water. The results suggest that the polymer has an almost non-polar surface, which can have significant implications for its applications in various fields, such as coatings and adhesives.

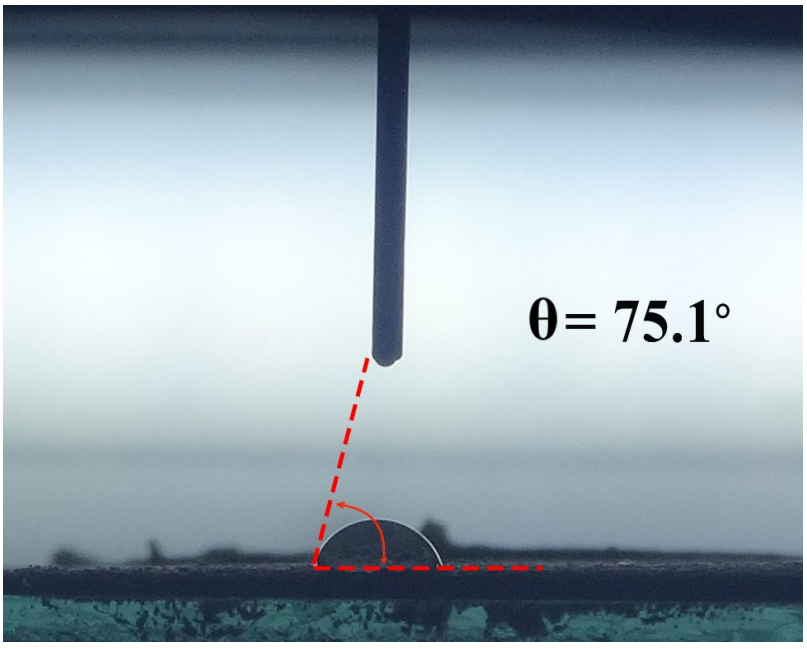

Fig. 6. Contact angle image of final UPR

Comparative study of presented UPR

In a comparison study of the mechanical properties of the present UPR with other works, Heat Deflection Temperature (HDT), Tensile Strength, Flexural Strength, and Sandability tests were conducted. According to Table 1, In terms of HDT, present UPR has shown to have a Relatively higher or competitive HDT compared to other materials. This indicates that our resin can withstand higher temperatures without losing its structural integrity, making it suitable for applications that require thermal stability. When it comes to Tensile Strength, present UPR has outperformed other materials in terms of its ability to withstand tension without breaking or deforming. This makes our resin a reliable choice for applications that require high tensile strength. Similarly, in the Flexural Strength test, present UPR has exhibited better performance compared to other works. Its ability to resist bending and flexing without fracturing or deforming makes it a durable and reliable material for various applications.

Table 1. Comparison of mechanical properties of different Resins (clear casting)

product	Tensile Strength	Flexural Strength	HDT	Barcool Hardness
Present UPR	65	100	75	42
Other work [36]	66		75	35
Other work [37]	40	53	69	
Other work [38]	45	89		

Specimen tested cured as follows: 24 hrs @20 °C, 5 hrs @ 80 °C, 3 hrs @ 120 °C

Present UPR demonstrated better sanding performance (**Table 2**), exhibiting a notably shorter time for completion compared to other similar products. This finding underscores the better workability and sanding characteristics of present UPR, making it an ideal choice for manufacturers of car body putty.

Table 2. Comparison of different UPR in sanding test.

Entry	UPR	Sandable (min)
1	Present UPR	After 15 min
2	Xylene Formaldehyde UPR	After 120 min [39]
3	DCPD UPR	After 20 min [40]

3. Conclusions

In Conclusion, a novel synthesis method for the development of a new HUPR was presented. The modification of DCOFA with MMA, styrene, DCPD-M and TMPDE resulted in the successful synthesis of a hyperbranched resin with improved properties. The synthesized resin exhibited enhanced thermal stability, mechanical properties, and potential applications in the polymer industry.

Acknowledgements

Partial financial support of University of Guilan and Nano Polymer Davam Shimi (NPDSCO) for this research work is sincerely acknowledged.

4. Experimental

4.1. Materials and Methods

DCOFA with an acid value of 198 mg KOH/g and DCPD were supplied by Arvalli Castor Derivatives Private Limited, Gujarat, India. MMA was supplied by Jin Dun chemical, China. TMPDE Supplied from Zhuhai Feiyang Novel Materials Corporation Limited, Zhuhai, Guangdong, China. Styrene was supplied by pars petrochemical, Iran. Tertiary butyl per benzoate (TBPB) was supplied by Akzonobel, Netherlands. PETN and MA were supplied by Fengchen Group, China. Hydroquinone (HQ) and p-tolyldiethanolamine (p-tolyl) were supplied from Sigma-Aldrich Chemie GmbH, Taufkirchen, Germany. Copper octoate ($Cu(oct)_2$) and Paraffin were supplied from local place.

FT-IR spectra were recorded on Thermo Nicolet Nexus 670 spectrophotometer using the KBr-pellet technique. Scanning electron microscope (SEM) measurements were recorded on a model: VP 1450, company: LEO-Germany. Gel Permeation Chromatography (GPC) measurements were performed on a model: Watters 1515, company: USA. The storage modulus of composites was analyzed using a dynamic mechanical analyzer (TA Instruments, Q800 DMA, New Castle, DE, USA) over a temperature range of 0 to 150 °C, with a fixed frequency of 1 Hz and heating rate of 10 °C·min^{-1}. The wettability of the surface was tested by measuring the contact angle using a ZAM104-B (Zolalan Sharif Pars Instruments, Iran). The tensile tests were performed on STM-20 at a fixed crosshead speed of 2mm min^{-1}. Samples were prepared according to ISO 527-2-2012. Flexural tests were done on STM-20 at a fixed crosshead speed of 2mm min^{-1}. Samples were prepared according to ISO 178:2019

4.2. General procedure

4.2.1. Preparation of modified DCOFA with MMA and Styrene (Intermediate A)

96 g (0.958 mol) of MMA, 96 g (0.921 mol) of Styrene and 14 g (0.072 mol) of TBPB are mixed at room temperature and then through a dropping funnel added drop wisely to the 57.6 g (0.192 mol) of DCOFA at 130 ºC over 2 hours in the reflux condition. After 2 hours and at the end of the injection of monomers, added another 1 g (5 mmol) of TBPB drop wisely through a dropping funnel at 130 ºC over 10 min in the reflux condition, Subsequently, a vacuum pump was employed to gradually create a vacuum pressure of 0.7 bar within the flask, which was placed under a nitrogen blanket and subjected to continuous stirring. This process continued until all unreacted monomers were effectively extracted from the mixture, mixture is then cooled to 50 °C.

4.2.2. Preparation of modified DCPD-M (Intermediate B)

In a 1000 mL three-necked round-bottom flask equipped with a condenser, thermometer and a magnetic stirrer, add 160 g (1.63 mol) of MA and 35.7 g (1.98 mol) of water. Heat the mixture to 80°C under constant stirring until the MA dissolves completely. Add 289.2 g (2.187 mol) of DCPD dropwise to the reaction mixture over 2 hours while maintaining the temperature at 80°C. After the addition is complete, continue stirring the reaction mixture for an additional 2 hours.

4.2.3. Preparation of final UPR

In the subsequent step, Intermediate A and 14.7 g (0.108 mol) of Pentaerythritol (PETN) were added into the mixture obtained from the second step (Intermediate B), within a flask placed under a nitrogen blanket while stirring. The mixture was then heated gradually to 200°C over a period of 3 hours. The reaction proceeded until the acid value of the resin dropped below 75 mg KOH/g. Following this, a dropwise addition of 236.75 g (1.1 mol) of TMPDE took place over a span of 2 hours. As the acid value of the resin reached below 40 mg KOH/g, a vacuum pump was employed to gradually establish a vacuum pressure of 0.7 bar within the flask, while stirring under a nitrogen blanket. Once the acid value of the resin reached 16 mg KOH/g, the mixture was cooled down to 175°C. Subsequently, 0.25 g (2.2 mmol) of HQ and 0.6 g of paraffin were added to the mixture. In the subsequent step, the mixture was gradually introduced into 410 g of styrene. It is important to ensure that the temperature of the mixture does not exceed 60 °C during this addition process. Finally, 0.03 g (0.08 mmol) of Cu(oct)2 and 0.6 g (3 mmol)of p-tolyl were incorporated into the mixture as the last step (**Scheme 4**).

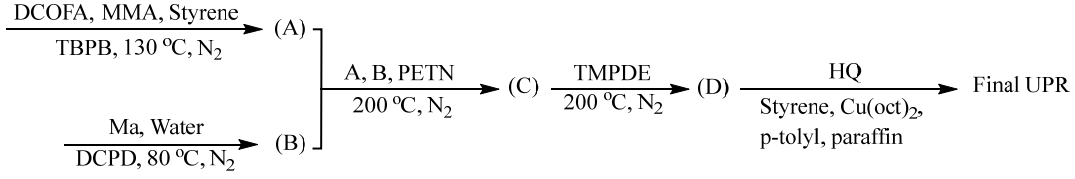

Scheme 4. Synthesis route for preparation of final UPR

Hydroquinone (HQ), a well-known inhibitor, is often employed in UPR systems to regulate the gel time during the curing process. By controlling the polymerization kinetics, HQ helps to fine-tune the curing duration. Its role as an inhibitor is important in preventing premature gelation, thereby allowing for sufficient time for the material to be processed and shaped before solidifying. P-tolyl plays a crucial role in UPR curing process, when used in combination with benzoyl peroxide. Benzoyl peroxide is a widely used initiator in the curing process of UPR. However, it requires an activator to initiate the radical reaction that leads to the crosslinking of the resin. P-tolyl serves as an activator or co-catalyst in the curing process. When combined with benzoyl peroxide, it facilitates the decomposition of the peroxide, leading to the generation of free radicals. These free radicals, in turn, initiate the polymerization reaction of the UPR with styrene, promoting the formation of a crosslinked network. $Cu(oct)_2$ known for its role in increasing the shelf life of UPR products. This organic copper salt acts as a stabilizer, effectively extending the storage duration of UPR by inhibiting premature polymerization. By controlling the oxidation and cross-linking reactions within the resin, $Cu(oct)_2$ helps to maintain the resin's usability over an extended period, thereby reducing waste and ensuring product quality.

UPR added to the styrene monomer at the final step to allow for the polymerization of the styrene monomer with the unsaturated bond in UPR chain in the mixture. This can lead to the formation of a block copolymer, where the UPR units are linked to the styrene units, resulting in a unique material with improved properties compared to the individual polymers. In this process, no specific separation or purification is carried out before adding the polyester to styrene. All the polyester produced is directly dissolved in the styrene.

4.2.4. Preparation of Automobile Body Putty

To ensure easy application and achieve a smooth and uniform surface, the putty needs to possess certain characteristics. It should facilitate the sanding process, allowing for easier refinement. In this study, a body putty mixture was formulated by combining specific ingredients with the UPR under vacuum and with agitation. The mixture consisted of 40 g of UPR, 60 g of talk, 0.3 g of dispersing agent, 0.5 g of bentonite, 2.8 g of titanium dioxide, and 1 g of fumed silica. The vacuum condition during agitation played a crucial role in breaking down internal resistance and allowing air bubbles to rise to the surface and eventually dissipate. Once the putty mixture was prepared, it was further mixed with a 2% concentration of 50% active BPO catalyst paste. This catalyzed putty was then applied to the sheet metal surface. After approximately 10 min, the applied putty was left to dry, and after 15 min, it became ready for sanding. By following this procedure, the putty could be easily applied to achieve a regular and homogeneous surface. Additionally, the putty's composition and the vacuum agitation helped in eliminating air bubbles and enhancing the overall quality of the final surface.

4.2.5. Chemical and mechanical properties of UPR

Table 3 presents the comprehensive results of the chemical and mechanical properties of the UPR under investigation. The UPR samples were subjected to various tests to evaluate their performance in terms of chemical properties, mechanical strength, and other key properties.

Table 3. Chemical and mechanical properties of final UPR

Entry	Properties	Unit	Final UPR	Test method	Ref
1	Appearance	----	opaque	----	
2	Color	Gardner	Min10	ASTM D-1544-98	[41]
3	Viscosity [a]	cP	550	ISO 2555:2000	[42]
4	Acid number	mgKOH/g	16	ASTM D-1639	[43]
5	Solid content	% weight	65	ASTM D-1259	[44]
6	Gel time [b]	Min	8	ASTM D2471-99	[45]
7	Tensile strength	MPa	65	ISO 527-2-2012	[46]
8	Flexural strength	MPa	100	ISO 178-2019	[47]
9	Heat distortion temp.	°C	75	ASTM D-648	[48]
10	Hardness Barcol		42	ASTM D2583	[49]
11	Linear shrinkage (ΔL\L)	%	0.8	ASTM – D2566	[50]

[a] (Brookfield RV, #3 60 rpm, 25 °C) [b] Gel time terms: 2% Benzoyl peroxide paste 50%

TGA Analysis

TGA was done on an SDT Q600 V20.9 build 20 thermal analyzer with a heating rate of 10 °C min -1. The TGA obtained for Final UPR is shown in **Fig. 7**. **Fig. 7 (a)** shows that the aging process starts at 250°C and continues up to 350°C, accompanied by a weight loss of about 50%.

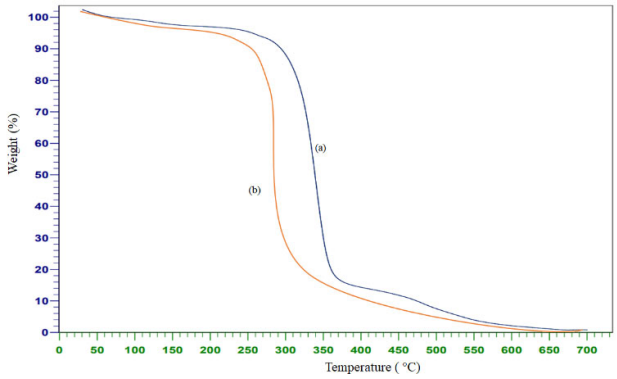

Fig. 7. TGA graph of final UPR, (a) in N_2, (b) in air

During this aging process, the UPR experiences weight loss, which is expected. This weight loss indicates the decomposition of certain components and the release of volatile substances from the resin structure (**Fig. 7 (a)**). A weight loss of about 50% at above 250 ºC indicates that UPR can undergo a moderate degree of thermal degradation without compromising its overall integrity or performance. These findings highlight the importance of considering the temperature limits for the UPR application, as prolonged exposure to temperatures above 350°C may lead to further weight loss and potentially impact the resin's properties. Also, the degradation behaviors of the samples were found to differ significantly when tested in an oxidative atmosphere (air), as compared to nitrogen. This suggests that the absence of oxygen had a noticeable impact on the thermal degradation behaviors of the samples. This observation suggests that the presence of oxygen can accelerate acid-catalyzed cross-linking actions during polymer degradation (**Fig. 7 (b)**).

References

1. Wooley K. L., Hawker C. J., Lee R., and Fréchet J. M. J. **(1994)** One-step synthesis of hyperbranched polyesters. Molecular weight control and chain end functionalization. *Polym. J*, 26(2), 187-197. (DOI: 10.1295/polymj.26.187)
2. Wooley K. L., Fréchet J. M., and Hawker, C. J. **(1994)** Influence of shape on the reactivity and properties of dendritic, hyperbranched and linear aromatic polyesters. *Polymer*, 35(21), 4489-4495. (DOI: 10.1016/0032-3861(94)90793-5)
3. Abdollahi M., and Khalili, B. **(2024)** Advancements in polyurethane coating: Synthesis and characterization of a novel hyper branched polyester polyol. *Curr. Chem. Lett*, 13(1), 117-126. (DOI: 10.5267/j.ccl.2023.8.004)
4. Turner S. R., Voit B. I., and Mourey, T. H. **(1993)** All-aromatic hyperbranched polyesters with phenol and acetate end groups: synthesis and characterization. *Macromol*, 26(17), 4617-4623. (DOI: 10.1021/ma00069a031)
5. Gao C., and Yan, D. **(2004)** Hyperbranched polymers: from synthesis to applications. *Prog. Polym. Sci*, 29(3), 183-275. (DOI: 10.1016/j.progpolymsci.2003.12.002)
6. Jikei M., and Kakimoto, M. A. **(2001)** Hyperbranched polymers: a promising new class of materials. *Prog. Polym. Sci*, 26(8), 1233-1285. (DOI: 10.1016/s0079-6700(01)00018-1)
7. Seiler, M. **(2006)** Hyperbranched polymers: Phase behavior and new applications in the field of chemical engineering. *Fluid Ph. Equilibria*, 241(1-2), 155-174. (DOI: 10.1002/chin.200634270)
8. Yates C. R., and Hayes, W. **(2004)** Synthesis and applications of hyperbranched polymers. *Eur. Polym. J*, 40(7), 1257-1281. (DOI: 10.1016/j.eurpolymj.2004.02.007)
9. Feng L., Li R., Yang H., Chen S., and Yang, W. **(2022)** The Hyperbranched Polyester Reinforced Unsaturated Polyester Resin. *Polymers*, 14(6), 1127. (DOI:10.3390/polym14061127)
10. Keinänen K., and Wigington G. **(2001)** Unsaturated polyester resins: U.S. Patent 6,268,464.
11. Russell R. F. **(1983)** Unsaturated polyester resins: U.S. Patent 4,387,171
12. Hamer G. D., and Russell R.F. **(1982)** Unsaturated polyester resins: U.S. Patent 4,336,169.
13. Weil E. D., and Levchik, S. V. **(2004)** Commercial flame retardancy of unsaturated polyester and vinyl resins. *J. Fire Sci*, 22(4), 293-303. (DOI:10.1177/0734904104041210)
14. Seraji S. M., Song P., Varley R. J., Bourbigot S., Voice D., and Wang, H. **(2022)** Fire-retardant unsaturated polyester thermosets: The state-of-the-art, challenges and opportunities. *Chem. Eng. J*, 430, 132785. (DOI: 10.1016/j.cej.2021.132785)
15. Hai Y., Jiang S., Zhou C., Sun P., Huang Y., and Niu, S. **(2020)** Fire-safe unsaturated polyester resin nanocomposites based on MAX and MXene: A comparative investigation of their properties and mechanism of fire retardancy. *Dalton trans*, 49(18), 5803-5814.(DOI: 10.1039/d0dt00686f)
16. Huang X., Yan X. M., Chen W. J., Tan C. Y., Yin G. Q., and Feng, G. Z. **(2021)** C36 Dimer Fatty Acid-Based Flexible Unsaturated Polyester Resin: Improvement of Properties by Adjusting the Intermolecular Crosslinking Structure. *Sci. Adv. Mater*, 13(4), 597-607. (DOI: 10.1166/sam.2021.3933)
17. Dholakiya B. **(2012)** Unsaturated Polyester Resin for Specialty Applications. London.
18. Uz Zaman S., Shahid S., Shaker K., Nawab Y., Ahmad S., Umair M., ... and Azam, F. **(2022)** Development and characterization of chemical and fire resistant jute/unsaturated polyester composites. *J. Text. Inst*, 113(3), 484-493. (DOI: 10.1080/00405000.2021.1889131)
19. Liu L., Xu Y., Xu M., He Y., Li S., and Li, B. **(2020)** An efficient synergistic system for simultaneously enhancing the fire retardancy, moisture resistance and electrical insulation performance of unsaturated polyester resins. *Mater. Des*, 187, 108302. (DOI: 10.1016/j.matdes.2019.108302)

20. Monti M., Natali M., Petrucci R., Kenny J. M., and Torre, L. **(2011)** Carbon nanofibers for strain and impact damage sensing in glass fiber reinforced composites based on an unsaturated polyester resin. *Polym. Compos*, 32(5), 766-775. (DOI: 10.1002/pc.21098)
21. Rahman M. T., Hoque M. A., Rahman G. T., Gafur M. A., Khan R. A., and Hossain, M. K. **(2019)** Study on the mechanical, electrical and optical properties of metal-oxide nanoparticles dispersed unsaturated polyester resin nanocomposites. *Results Phys*, 13, 102264. (DOI: 10.1016/j.rinp.2019.102264)
22. Chu F., Qiu S., Zhou Y., Zhou X., Cai W., Zhu Y., ... and Hu, W. **(2022)** Novel glycerol-based polymerized flame retardants with combined phosphorus structures for preparation of high performance unsaturated polyester resin composites. *Compos. B: Eng*, 233, 109647. (DOI: 10.1016/j.compositesb.2022.109647)
23. Pistone A., Visco A. M., Galtieri G., Iannazzo D., Espro C., Merlo F. M., ... and De Leo, F. **(2016)** Polyester resin and carbon nanotubes based nanocomposite as new-generation coating to prevent biofilm formation. *Int. J. Polym. Anal*, 21(4), 327-336. (DOI: 10.1080/1023666X.2016.1155826)
24. Sousa A. F., Fonseca A. C., Serra A. C., Freire C. S. R., Silvestre A. J. D., and Coelho, J. F. J. **(2016)** New unsaturated copolyesters based on 2, 5-furandicarboxylic acid and their crosslinked derivatives. *Polym. Chem*, 7(5), 1049-1058. (DOI: 10.1039/C5PY01702E)
25. Kim J., Jeong D., Son C., Lee Y., Kim E., and Moon, I. **(2007)** Synthesis and applications of unsaturated polyester resins based on PET waste. *Korean. J. Chem. Eng*, 24, 1076-1083. (DOI: 10.1007/s11814-007-0124-5)
26. Kirshanov K., Toms R., Melnikov P., and Gervald, A. **(2022)** Unsaturated Polyester Resin Nanocomposites Based on Post-Consumer Polyethylene Terephthalate. *Polymers*, 14(8), 1602. (DOI: 10.3390/polym14081602)
27. Bagheri K., Razavi S. M., Ahmadi S. J., Kosari M., and Abolghasemi, H. **(2018)** Thermal resistance, tensile properties, and gamma radiation shielding performance of unsaturated polyester/nanoclay/PbO composites. *Radiat. Phys. Chem*, 146, 5-10. (DOI: 10.1016/j.radphyschem.2017.12.024)
28. Singh B., Gupta M., Verma A., and Tyagi, O. S. **(2000)** FT-IR microscopic studies on coupling agents: treated natural fibres. *Polym. Int*, 49(11), 1444-1451. (DOI: 10.1002/1097-0126(200011)49:11<1444::AID-PI526>3.0.CO;2-9)
29. Paci M., Crescenzi V., and Campana, F. **(1982)** Magic Angle Spinning-Cross Polarization 13 C NMR of crosslinked unsaturated polyester resins. *Polym. Bull*, 7, 59-63. (DOI: 10.1007/BF00265452)
30. Han C. D., and Lee, D. S. **(1987)** Analysis of the curing behavior of unsaturated polyester resins using the approach of free radical polymerization. *J. Appl. Polym. Sci*, 33(8), 2859-2876. (DOI: 10.1002/app.1987.070330820)
31. Yang Y. S., and Lee, L. J. **(1988)** Microstructure formation in the cure of unsaturated polyester resins. *Polymer*, 29(10), 1793-1800. (DOI: 10.1016/0032-3861(88)90393-X)
32. Hsu C. P., and Lee, L. J. **(1991)** Structure formation during the copolymerization of styrene and unsaturated polyester resin. *Polymer*, 32(12), 2263-2271. (DOI: 10.1016/0032-3861(91)90057-P)
33. Chen J. S., and Yu, T. L. **(1998)** Microgelation of unsaturated polyester resins by static and dynamic light scattering. *J. Appl. Polym. Sci*, 69(5), 871-878. (DOI: 10.1002/(SICI)1097-4628(19980801)69:5<871::AID-APP5>3.0.CO;2-J)
34. karak N. **(2012)** 4 - Vegetable oil-based polyesters,Vegetable Oil-Based Polymers, Woodhead Publishing. 96-125. (DOI: 10.1533/9780857097149.96)
35. Perrot A., Hyršl J., Bandžuch J., Waňousová S., Hájek J., Jenčík J., and Herink, T. **(2021)** Use of dicyclopentadiene and methyl dicyclopentadiene for the synthesis of unsaturated polyester resins. *Polymers*, 13(18), 3135. (DOI: 10.3390/polym13183135)
36. Azzouz L. **(2021)** Development and Characterisation of Novel Biocomposites Fabricated Using Natural Fibres and Rapid Prototyping Technology. Pages 84-85
37. Qin C., Jin Q., Zhao J., Wang Y., and Jiang C. **(2023)** Study on the Mechanical Characteristics, Heat Resistance, and Corrosion Resistance of Unsaturated Polyester Resin. *Compos. Struct*, 13(7), 1700. (DOI: 10.3390/buildings13071700).
38. Feng L., Li R., Yang H., Chen S., and Yang, W. **(2022)** The Hyperbranched Polyester Reinforced Unsaturated Polyester Resin. *Polymers*, 14(6), 1127. (DOI: 10.3390/polym14061127)
39. Liu F. F., Feng Q. N., Yuan X. H., and Liu, X. W. **(2014)** The Synthesis of Xylene Formaldehyde Unsaturated Polyester Resin and Its Application in the Putty. *Adv. Mat. Res*, 1051, 294-298. (DOI:10.4028/www.scientific.net/AMR.1051.294.
40. Ruggeberg D. A. **(1995)** European Patent No. 0739369A1.
41. ASTM D1544-04 **(2018)**. Standard Test Method for Color of Transparent Liquids (Gardner Color Scale). Annual Book of Standards.
42. ISO 2555 **(2018)**. Plastics — Resins in the liquid state or as emulsions or dispersions Determination of apparent viscosity using a single cylinder type rotational viscometer method.
43. ASTM D1639-90 **(1996)** standard test method for acid value of organic coating materials Annual Book of Standards.
44. ASTM D1259-06 **(2018)** Standard test methods for nonvolatile content of resin solutions Annual Book of Standards.
45. ASTM D2471-99 **(2008)** Standard test method for gel time and peak exothermic temperature of reacting thermosetting resins Annual Book of Standards.
46. ISO 527-2 **(2012)** Plastics — Determination of tensile properties — Part 2: Test conditions for moulding and extrusion plastics.
47. ISO 178 **(2019)** Plastics — Determination of flexural properties.
48. ASTM D648-18 **(2016)** Standard test method for deflection temperature of plastics under flexural load in the edgewise position Annual Book of Standards.
49. ASTM D2583-13a **(2022)** Standard test method for indentation hardness of rigid plastics by means of a barcol impressor Annual Book of Standards.
50. ASTM D2566 **(1993)** Standard test method for linear shrinkage of cured thermosetting casting resins during cure Annual Book of Standards